Whistler Turbulence Wavevector Anisotropies: Particle-in-cell Simulations

S. Peter Gary

Los Alamos National Laboratory, Los Alamos, NM 87545

pgary@lanl.gov

Shinji Saito

Solar-Terrestrial Environment Laboratory, Nagoya University, Nagoya, Aichi 464-8601

Japan

saito@stelab.nagoya-u.ac.jp

and

Yasuhito Narita

Institute of Geophysics and Extraterrestrial Physics, Technical University of Braunschweig,

D-38106 Braunschweig, Germany

y.narita@tu-bs.de

Received _____; accepted _____

Submitted to Astrophysical Journal

ABSTRACT

Two-dimensional electromagnetic particle-in-cell simulations of whistler turbulence in a magnetized, homogeneous, collisionless plasma of electrons and protons are carried out. Enhanced magnetic fluctuation spectra are initially imposed at relatively long wavelengths, and, as in previous such simulations, the temporal evolution shows a forward cascade of magnetic fluctuation energy to shorter wavelengths, with more fluctuation energy at a given wavenumber perpendicular to $\mathbf{B}_o$ than at the same wavenumber parallel to the background field. The new result here is that the wavevector anisotropy is very different for each of the three components of the fluctuating magnetic field. Here $\|$ denotes the direction parallel to the background magnetic field $\mathbf{B}_o$, $\perp$ indicates the direction perpendicular to $\mathbf{B}_o$ and in the simulation plane, and the symbol $\perp\perp$ denotes the direction perpendicular to both $\mathbf{B}_o$ and the simulation plane. The anisotropy angle of the jth magnetic component is defined as

$$\tan^2\theta_{Bj} \equiv \frac{\Sigma_k\ k_\perp^2 |\delta B_j(k_\|, k_\perp)|^2}{\Sigma_k\ k_\|^2 |\delta B_j(k_\|, k_\perp)|^2}$$

Then the simulations show that $\tan^2\theta_{B\|} >> 1$, $\tan^2\theta_{B\perp} > 1$, and $\tan^2\theta_{B\perp\perp} < 1$.

Subject headings: turbulence; electron-positron plasmas; dissipation

1. Introduction

Single-spacecraft measurements of plasma turbulence in the solar wind yield magnetic fluctuation spectra at observed frequencies $f' \lesssim 0.2$ Hz that scale as $(f')^{-5/3}$ [*Smith et al.*, 2006; *Podesta et al.*, 2007]; this is called the "inertial range." In the range 0.2 Hz $\lesssim f' \lesssim$ 0.5 Hz, measurements near 1 AU further show a spectral breakpoint, a distinct change to spectra that are steeper than those of the inertial range [*Leamon et al.*, 1998; *Smith et al.*, 2006; *Alexandrova et al.*, 2008]. At higher observed frequencies, magnetic spectra exhibit steeper power laws, i.e., $|\delta\mathbf{B}(f')|^2 \sim (f')^{-\alpha_f}$ with $1.8 \lesssim \alpha_f \lesssim 4.5$ [*Behannon*, 1978; *Denskat et al.*, 1983; *Goldstein et al.*, 1994; *Lengyel-Frey et al.*, 1996; *Leamon et al.*, 1998; *Bale et al.*, 2005; *Smith et al.*, 2006]. Recent analyses of measurements from the multi-spacecraft Cluster mission have extended such measurements to $f' \lesssim 100$ Hz, showing that spectra in this range scale with $2 < \alpha_f < 3$ [*Sahraoui et al.*, 2009; *Kiyani et al.*, 2009; *Alexandrova et al.*, 2009].

Although inertial range turbulence corresponds to relatively large fluctuation levels ($|\delta\mathbf{B}|^2 \lesssim B_o^2$) where $\mathbf{B}_o$ denotes an average, uniform background magnetic field, high frequency turbulence above the spectral breakpoint is relatively weak ($|\delta\mathbf{B}|^2 << B_o^2$). So this regime may be thought of as an ensemble of weakly interacting fluctuations which are individually described by linear dispersion theory. In this framework, there are two competing hypotheses as to the character of the normal modes in this regime. One scenario is that this turbulence consists of kinetic Alfvén waves which propagate in directions quasi-perpendicular to $\mathbf{B}_o$ and at real frequencies $\omega_r < \Omega_p$, the proton cyclotron frequency. Both solar wind observations [*Leamon et al.*, 1998; *Bale et al.*, 2005; *Sahraoui et al.*, 2009] and gyrokinetic simulations [*Howes et al.*, 2008a; see also *Matthaeus et al.*, 2008, and *Howes et al.*, 2008b] of turbulence above the spectral breakpoint have been interpreted as consisting of such normal modes, although it is unlikely that kinetic Alfvén waves represent

the full physics of such turbulence in the solar wind [*Gary and Smith*, 2009; *Shaikh and Zank*, 2009; *Podesta et al.*, 2010]. A second hypothesis is that whistler fluctuations at $\Omega_p < \omega_r < \Omega_e$ (where the latter symbol represents the electron cyclotron frequency) are the fundamental modes of turbulence above the breakpoint. Such modes are often observed in the solar wind [*Beinroth and Neubauer*, 1981; *Lengyel-Frey et al.*, 1996] and recent particle-in-cell (PIC) simulations have demonstrated that such modes can cascade to relatively short wavelengths and thereby develop turbulent magnetic spectra with relatively steep power-law wavenumber dependence [*Gary et al.*, 2008; *Saito et al.*, 2008; *Svidzinski et al.*, 2009].

In the framework of the second scenario, we here use PIC simulations to extend the computations of *Saito et al.* [2008] and to examine further properties of cascading whistler turbulence. As in that paper, the computations described here utilize a two-dimensional, fully relativistic, collisionless particle-in-cell electromagnetic simulation code [*Buneman*, 1993]. Here "two-dimensional" means that the simulation allows variations in two spatial dimensions, $\hat{\mathbf{x}}$, the direction parallel to $\mathbf{B}_o$, and $\hat{\mathbf{y}}$, perpendicular to the background magnetic field. The subscripts x and $\|$ are equivalent, as are the subscripts y and $\perp$. Note that, because our simulations are two-dimensional, $\perp$ denotes a Cartesian, rather than a cylindrical, coordinate. We futher use the symbol $\perp\perp$ to denote the $\hat{\mathbf{z}}$ direction which is perpendicular to both $\mathbf{B}_o$ and the simulation plane.

The code calculates the full three-dimensional velocity space response of each proton and electron superparticle throughout the simulations. The plasma is homogeneous with periodic boundary conditions. The number of superparticles per cell is 64, the system has spatial dimensions $L_x = L_y = 102.4c/\omega_e$ where c/ω_e is the electron inertial length, the time step is $\delta t = 0.05/\omega_e$, and the grid spacing is $\Delta = 0.10c/\omega_e$. For these parameters, the fundamental mode of the simulation has wavenumber $kc/\omega_e = 0.0613$, and short wavelength

fluctuations are resolved up to the component wavenumber of $k_j c/\omega_e = 4$. The initial physical dimensionless parameters are $m_p/m_e = 1836$, $T_e/T_p = 1.0$, $\beta_p = 0.10$, and $\omega_e^2/\Omega_e^2 = 5.0$, where the symbols are as defined in *Gary* [1993]. For these parameters, $v_e/c = 0.10$, so that the electron temperature is about 2.5 keV.

We initially impose 42 right-hand polarized whistler waves at $t = 0$. Initial wavenumbers are $k_\parallel \lambda_e = \pm 0.0613$, ± 0.1227, and ± 0.184, and $k_\perp \lambda_e = 0, \pm 0.0613$, ± 0.1227, and ± 0.184. The frequencies are derived from the linear dispersion relation for magnetosonic-whistler fluctuations in a collisionless plasma with the same parameters as shown above. Each wave has an equal fluctuating magnetic energy at $t = 0$. Given the initial magnetic fluctuations $\delta\mathbf{B}_n$, the initial $\delta\mathbf{E}_n$ and $\delta\mathbf{J}_n$ satisfy Faraday's and Ampere's equations, where the subscript "n" is a mode number from 1 to 42 for the initial fluctuations. The phases of each mode are chosen randomly.

We define the reduced magnetic fluctuation energy spectra as

$$|\delta\mathbf{B}(k_\parallel)|^2 \equiv \Sigma_{k_\perp} |\delta\mathbf{B}(k_\parallel, k_\perp)|^2$$

and

$$|\delta\mathbf{B}(k_\perp)|^2 \equiv \Sigma_{k_\parallel} |\delta\mathbf{B}(k_\parallel, k_\perp)|^2$$

We further define the fitting parameters $\alpha_\parallel$ and $\alpha_\perp$ by

$$|\delta\mathbf{B}(k_j)|^2 = C k_j^{-\alpha_j} \qquad j = \parallel, \perp$$

2. Simulation Results

We have done four simulations in which the only initial parameter which is varied is the initial fluctuation energy $\epsilon_B \equiv \sum_{n=1}^{42} |\delta\mathbf{B}_n(t=0)|^2/B_o^2$, where $|\delta\mathbf{B}_n|^2 = \sum_{j=x,y,z} |\delta B_{j,n}|^2$. The simulations correspond to $\epsilon_B = 0.05$, 0.1, 0.2, and 0.5, where the first two runs emulate the corresponding runs of *Saito et al.* [2008].

All of these simulations qualitatively reproduce the results of *Saito et al.* [2008]. The initial, long-wavelength fluctuations yield a forward cascade in which the energy is transferred to shorter wavelengths; the cascade leads to fluctuation energy being preferentially transferred to $k_\perp$; and, as a result, $\alpha_\perp << \alpha_\parallel$. Figure 1 shows that $\alpha_\perp$ becomes smaller as each simulation progresses, and $\alpha_\perp$ becomes smaller with increasing ϵ_B. Thus the longer the simulation is run, and the more strongly the turbulence is driven, the flatter the spectra become and the more energy is cascaded to short wavelengths. These results suggest that large-amplitude, late-time simulations yield an asymptotic state which may provide a basis of comparison against the predictions of various models of whistler turbulence. For the simulations described here, Figure 1 indicates that this asymptotic state corresponds to $\alpha_\perp \lesssim 3$.

Fig. 4 of *Saito et al.* [2008] indicates that, at quasi-perpendicular propagation,

$$|\delta B_\parallel|^2 \sim |\delta B_{\perp\perp}|^2 >> |\delta B_\perp|^2$$

Figure 2 demonstrates that, even when we sum over all wavenumbers, this relationship remains approximately valid.

To quantify the anisotropy of whistler turbulence, we follow *Shebalin et al.* [1983] and *Saito et al.* [2008] and define the wavevector anisotropy angle θ_B by

$$\tan^2\theta_B \equiv \frac{\Sigma_k\ k_\perp^2 |\delta\mathbf{B}(k_\parallel, k_\perp)|^2}{\Sigma_k\ k_\parallel^2 |\delta\mathbf{B}(k_\parallel, k_\perp)|^2} \tag{1}$$

Figure 3(a), from *Saito et al.* [2008], shows $\tan^2\theta_B$ as a function of time from the simulation with $\epsilon_B = 0.10$. This quantity attains a late-time average value of about 6 ($\theta_B \simeq 68^o$), reflecting the fundamental anisotropy of whistler turbulence favoring quasi-perpendicular propagation relative to the background magnetic field.

However, Fig. 4 of *Saito et al.* [2008] shows that, at quasi-perpendicular propagation, $|\delta B_\perp|^2/B_o^2$ becomes much smaller than the energy in the other two components of $\delta\mathbf{B}$, and,

as indicated by *Gary and Smith* [2009], that $\delta B_{\parallel}$ competes with $\delta B_{\perp}$ for quasi-perpendicular whistler fluctuations. This suggests that we define three more anisotropy angles θ_{B_j}:

$$\tan^2 \theta_{Bj} \equiv \frac{\Sigma_k \; k_{\perp}^2 |\delta B_j(k_{\parallel}, k_{\perp})|^2}{\Sigma_k \; k_{\parallel}^2 |\delta B_j(k_{\parallel}, k_{\perp})|^2} \qquad j = \parallel, \perp, \perp\perp \tag{2}$$

These three quantities are illustrated in Figure 3(b). The very weak in-plane perpendicular component $\delta B_{\perp}$ is anisotropic in the sense of having more energy at quasi-parallel propagation than at quasi-perpendicular propagation. This is consistent with the condition $\nabla \cdot \mathbf{B} = 0$, which, when $k_{\parallel} = 0$, imposes $\delta B_{\perp} = 0$. The other two magnetic fluctuation components are anisotropic in the opposite sense: $\delta B_{\perp\perp}$ is moderately anisotropic at late times with $\tan^2\theta_B \simeq 6$, whereas the compressive component $\delta B_{\parallel}$ is strongly anisotropic with $\tan^2\theta_B \simeq 14$ at late times, corresponding to $\theta_B \simeq 75^o$.

3. Conclusions

We carried out two-dimensional particle-in-cell simulations of whistler turbulence in a homogeneous collisionless plasma of electrons and protons with a uniform background magnetic field $\mathbf{B}_o$. We imposed an initial spectrum of relatively long wavelength whistler fluctuations; as in previous such simulations there is a forward cascade of the fluctuating magnetic field energy to a shorter wavelength regime of whistler turbulence. The late-time turbulence is anisotropic with more fluctuation energy at a given wavenumber perpendicular to $\mathbf{B}_o$ than at the same wavenumber parallel to the background field. The new result here is that the wavevector anisotropy is strongest in the compressive component (i.e., the component of $\delta\mathbf{B}$ parallel to $\mathbf{B}_o$); the magnetic field component perpendicular to $\mathbf{B}_o$ and out of the simulation plane is moderately anisotropic, and the relatively weak magnetic component perpendicular to $\mathbf{B}_o$ is anisotropic in the opposite sense with more energy at quasi-parallel propagation than at quasi-perpendicular propagation. These results imply that analytic derivations of scaling relations for the properties of whistler turbulence should

not only distinguish differences between quasi-parallel and quasi-perpendicular propagation (i.e., scalings with $k_{\|}$ and $k_{\perp}$), as in *Saito et al.* [2008] and *Narita and Gary* [2010], but should also distinguish the different properties and contributions of the perpendicular and parallel fluctuating magnetic field components.

The power law characterizing late-time, large-amplitude spectra of whistler turbulence at quasi-perpendicular propagation is $\alpha_{\perp} \lesssim 3$, as indicated in Figure 1. This is a steeper power law than is predicted by scaling arguments for anisotropic whistler turbulence; for example, in a Cartesian coordinate system Equation (18) of *Narita and Gary* [2010] predicts

$$\frac{|\delta B|^2}{B_o^2} \sim \frac{1}{k_{\perp}^{3/2}} \tag{3}$$

The reason for this discrepancy is not clear. Perhaps the steeper spectra in the simulations are due to Landau damping of the whistlers. Or perhaps our simulations have not attained a fully asymptotic state; that is, perhaps a simulation at $\epsilon_B = 1.0$ would yield a still smaller late-time value of $\alpha_{\perp}$. A third possibility might be the need for modifications to the *Narita and Gary* [2010] derivation; for example, if the energy transfer rate $\epsilon_{\perp}$ is proportional to the fluctuating velocity energy $|\delta v|^2$, rather than the fluctuating magnetic energy $|\delta B|^2$, then the formalism of *Narita and Gary* [2010] yields

$$\frac{|\delta B|^2}{B_o^2} \sim \frac{1}{k_{\perp}^{5/2}} \tag{3}$$

which is much closer to the asymptotic result of the simulations.

In these two-dimensional simulations $k_{\perp\perp} = 0$, so that the turbulence is not gyrotropic, in contrast to what we would expect in a homogeneous physical system. Nevertheless, because our computations show both $|\delta B_{\perp}|^2$ and $|\delta B_{\perp\perp}|^2$ are much less anisotropic functions of wavenumber than $|\delta B_{\|}|^2$, we expect our primary conclusion, that the compressive component is much more anisotropic than the components perpendicular to $\mathbf{B}_o$, should remain valid in a fully three-dimensional simulation of homogeneous whistler turbulence.

The authors acknowledge useful exchanges with Joe Borovsky, John Podesta and Chuck Smith. The Los Alamos portion of this work was performed under the auspices of the U.S. Department of Energy (DOE). It was supported by the Solar and Heliospheric Physics SR&T and Heliophysics Guest Investigators Programs of the National Aeronautics and Space Administration.

REFERENCES

Alexandrova, O., V. Carbone, P. Veltri, and L. Sorriso-Valvo (2008), ApJ, *674*, 1153.

Alexandrova, O., J. Saur, C. Lacombe, A. Mangeney, J. Mitchell, S. J. Schwartz, and P. Robert (2009), Phys. Rev. Lett., *103*, 165003.

Bale, S. D., P. J. Kellogg, F. S. Mozer, T. S. Horbury, and H. Reme (2005), Phys. Rev. Lett., *94*, 215002.

Behannon, K. W. (1978), Revs. Geophys., *16*, 125.

Beinroth, H. J., and F. M. Neubauer (1981), J. Geophys. Res., *86*, 7755.

Buneman, O. (1993), Computer space plasma physics, in *Simulation Techniques and Software*, edited by H. Matsumoto and Y. Omura, P. 67, Terra Sci., Tokyo.

Denskat, K. U., H. J. Beinroth, and F. M. Neubauer (1983), J. Geophys., *54*, 60.

Gary, S. P., 1993, *Theory of Space Plasma Microinstabilities*, Cambridge University Press, New York.

Gary, S. P., and C. W. Smith (2009), J. Geophys. Res., *114*, A12105.

Gary, S. P., Saito, S., and Li, H., 2008, Geophys. Res. Lett., 35, L02104.

Goldstein, M. L., D. A. Roberts, and C. A. Fitch (1994), J. Geophys. Res., *99*, 11,519.

Howes, G. G., W. Dorland, S. C. Cowley, G. W. Hammett, E. Quataert, A. A. Schekochihin, and T. Tatsuno (2008a), Phys. Rev. Lett., *100*, 065004.

Howes, G. G., S. C. Cowley, W. Dorland, G. W. Hammett, E. Quataert, A. A. Schekochihin, and T. Tatsuno (2008b), Phys. Rev. Lett., *101*, 149502.

Kiyani, K. H., S. C. Chapman, Yu. V. Khotyaintsev, M. W. Dunlop, and F. Sahraoui (2009), Phys. Rev. Lett., *103*, 075006.

Leamon, R. J., C. W. Smith, N. F. Ness, W. H. Matthaeus, and H. K. Wong (1998), J. Geophys. Res., *103*, 4775.

Lengyel-Frey, D., R. A. Hess, R. J. MacDowall, R. G. Stone, N. Lin, A. Balogh, and R. Forsyth (1996), J. Geophys. Res., *101*, 27,555.

Matthaeus, W. H., S. Servidio, and P. Dmitruk (2008), Phys. Rev. Lett., *101*, 149501.

Narita, Y., and S. P. Gary (2010), Annales Geophys., *28*, 597.

Podesta, J. J., D. A. Roberts, and M. L. Goldstein (2007), ApJ, *664*, 543.

Podesta, J. J., J. E. Borovsky, and S. P. Gary (2010), ApJ, in press.

Sahraoui, F., M. L. Goldstein, P. Robert, and Yu. V. Khotyaintsev (2009), Phys. Rev. Lett., *102*, 231102.

Saito, S., Gary, S. P., Li, H., and Narita, Y., 2008, Phys. Plasmas, 15, 102305.

Shaikh, D., and G. P. Zank (2009), Mon. Not. R. Astron. Soc., *400*, 1881.

Shebalin, J. V., W. H. Matthaeus, and D. Montgomery (1983), J. Plasma Phys., *29*, 525.

Smith, C. W., K. Hamilton, B. J. Vasquez, and R. J. Leamon (2006), ApJ, *645*, L85.

Svidzinski, V. A., H. Li, H. A. Rose, B. J. Albright, and K. J. Bowers (2009), Phys. Plasmas, *16*, 122310.

Fig. 1.— The perpendicular power law index of the total energy density of the fluctuating magnetic fields as functions of time in each simulation.

Fig. 2.— Time histories of quantities summed over the cascading wavenumber range (0.3 $\leq |kc/\omega_e| \leq 3.0$) for the simulation with $\epsilon_B = 0$. (a) Total fluctuating magnetic field energy, and (b) fluctuating magnetic field component energies with $|\delta B_{\parallel}|^2/B_o^2$ denoted by the red line, $|\delta B_{\perp}|^2/B_o^2$ denoted by the blue line, and $|\delta B_{\perp\perp}|^2/B_o^2$ denoted by the green line.

Fig. 3.— Time histories of quantities summed over the cascading wavenumber range (0.3 $\leq |kc/\omega_e| \leq 3.0$) for the simulation with $\epsilon_B = 0$. (a) $\tan^2(\theta_B)$, and (b) $\tan^2(\theta_{B_{\parallel}})$ (red line), $\tan^2(\theta_{B_{\perp}})$ (blue line), and $\tan^2(\theta_{B_{\perp\perp}})$ (green line).

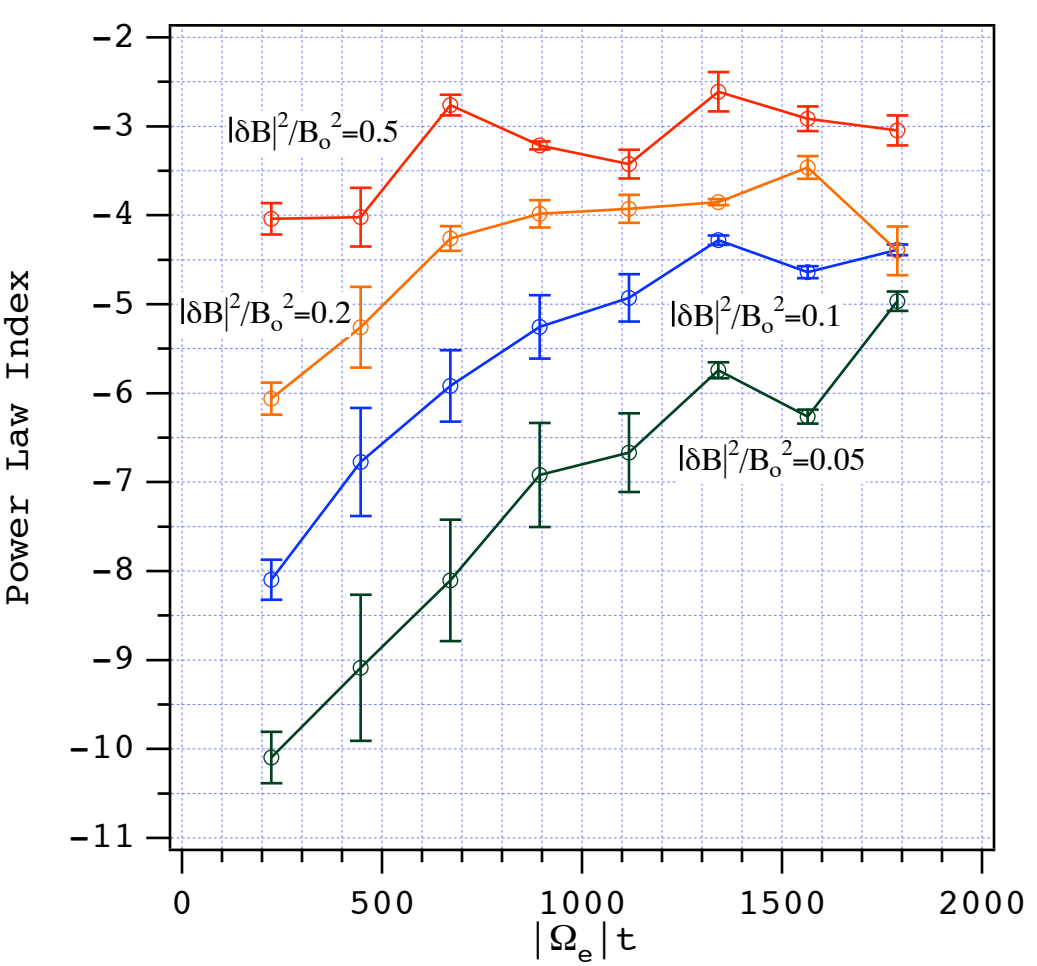
Power Law Index
−2
−3
−4
−5
−6
−7
−8
−9
−10
−11
0
500
1000
1500
2000
|Ωe|t
|δB|²/Bo²=0.5
|δB|²/Bo²=0.2
|δB|²/Bo²=0.1
|δB|²/Bo²=0.05

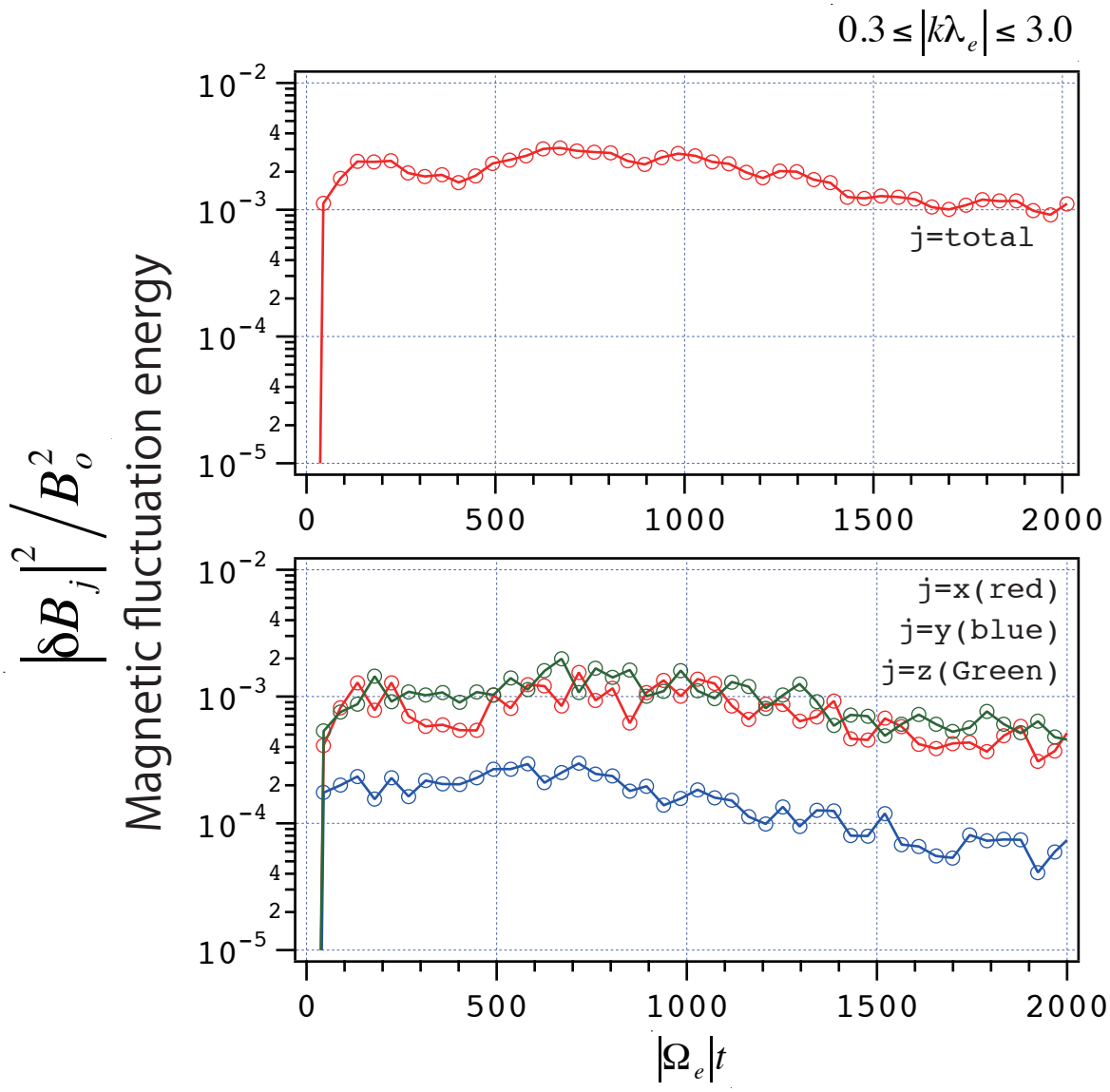
$0.3 \le |k\lambda_e| \le 3.0$
$|\delta B_j|^2 / B_o^2$
Magnetic fluctuation energy
j=total
j=x(red)
j=y(blue)
j=z(Green)
$|\Omega_e| t$

$$0.3 \le |k\lambda_e| \le 3.0$$

$$\tan^2\theta_{B_j} = \frac{\sum_k k_y^2 |B_j|^2}{\sum_k k_x^2 |B_j|^2}$$